URSI GASS 2020, Rome, Italy, 29 August - 5 September 2020

Long Term Rain Attenuation Measurements at Millimeter Wave Bands for Direct and Side Short-Range Fixed Links

O. Zahid, J. Huang, and S. Salous*
Department of Engineering, Durham University, Durham, DH1 3LE U.K., sana.salous@durham.ac.uk

Abstract

Millimeter wave (mmWave) radio links are largely affected by precipitation. In this paper, we use a custom-designed continuous wave (CW) channel sounder to record channel data at K band (25.84 GHz) and E band (77.52 GHz) for direct line of sight link and a side non line of sight link with dual polarizations. A high-performance PWS100 disdrometer is utilized to collect weather data, including rain rate and rain drop size distribution (DSD) for rain attenuation study. The rain attenuation for both links are compared. The side link exhibits a slightly higher attenuation than the direct link. The ITU-R P.838-3 model and DSD model are applied to model the rain attenuation. The results will be useful for the design of fixed links for fifth generation (5G) mmWave communication systems.

1 Introduction

MmWave communication is a key technology for 5G and short-range fixed links can be used for fronthaul, backhaul, and building to building transmission to provide high data transmission rate. A signal with frequency above 10 GHz can be affected by rain, which causes performance reduction and even outage of the communication system, especially at mmWave bands. Since rain is not uniform in space and time, long-term measurements over several years and various locations are needed. Its effects on mmWave propagation include absorption and scattering. Rain attenuation depends on the rain fall rate, rain drop size distribution, DSD, and complex water refractive index, which is related to the frequency band.

Several studies of rain attenuation at mmWave bands have been reported. For terrestrial links, most of the measurements are dedicated for long-range direct links where the transmitter (Tx) and receiver (Rx) antennas are in line-of-sight (LOS). In [1], a link was set up at 71-76 GHz over 1 km. The rain data were recorded by a visibility and precipitation optical sensor. The measured rain attenuation was shown to agree with the ITU-R P.838-3 model. In [2], a link was set up at 93 GHz with a link distance of 850 m. In [3], a link was set up at 38 GHz with over 1.85 km. The wet antenna attenuation was found to have a maximum value of 2.3 dB. In [4] and [5], a microwave link was set up at 72 GHz and 84 GHz with a link distance of 23.6 km. The rain data were recorded by an optical disdrometer. The results indicated that the ITU-R P.838 model may overestimate the rain attenuation. In [6], four microwave links were set up at 14.5 GHz with a distance range of 12.8-43 km and a new distribution model was proposed for the fade-slope statistics. In [7], a microwave link was set up at 26 GHz with a link distance of 1.3 km. The worst month statistic obtained from the real measurements was lower than what was predicted by the ITU-R P.581-2 model. In [8], a link was set up at 73, 83, 148, and 156 GHz with a link distance of 325 m. In [9], eight links were set up over a frequency range of 37.3-39.2 GHz with link distances of 48-497 m. The results showed different wet antenna attenuations for different rain rates, which indicated that the constant value of wet antenna attenuation used in some studies may overestimate the retrieved peak rain rates. In [10], five microwave links were set up at 32 GHz with link distances of 186-1810 m. The wet antenna attenuation was about 3 dB per antenna for a rain rate of 100 mm/h. In [11], a link was set up at 23, 25, 28, and 38 GHz with a link distance of 700 m. The results showed that the wet antenna effect, change of humidity level, and equipment stability would also impact the rain attenuation.

Compared to the above studies, our research concentrates on short-range building to building transmission scenarios. Both the LOS direct link and non-line-of-sight (NLOS) side links are set up at K band (25.84 GHz) and E band (77.52 GHz) with dual polarizations. The distance between the Tx and Rx is about 35 m for the direct link. The rain attenuation study for both links is then related to the ITU-R P.838-3 model using the rain fall rate and the DSD model with Mie scattering.

The remainder of this paper is organized as follows. Section 2 describes the measurement system setup. In Section 3, the rain attenuation models are introduced. The results and analysis are presented in Section 4. Finally, conclusions are drawn in Section 5.

2 Measurement System Setup

2.1 *Fixed link experimental setup*

The experimental setup reported in [12, 13] was updated as shown in Fig. 1 and in Fig. 2. Compared to the previous system, the intermediate frequency (IF) unit is replaced by a phase-locked loop (PLL) and integrated with the radio frequency (RF) heads into a single box to reduce the complexity of the system and enhance its stability.

In addition, the antennas which already had radomes are further covered to reduce the wet antenna effect. For the direct link, two antennas with vertical and horizontal polarizations are used for the E band, while a dual polarized antenna is used for the K band. For the side link receiver, single vertical polarized antennas are used for both bands. A 50 Hz trigger and 40 MHz clock are connected to the two data acquisition cards where the 50 Hz signal is also connected to the Tx to switch between vertical and horizontal polarizations and the 40 MHz provides the sampling clock. The IF signal to be digitized is set at 4 MHz and 12 MHz for the K band and E band, respectively.

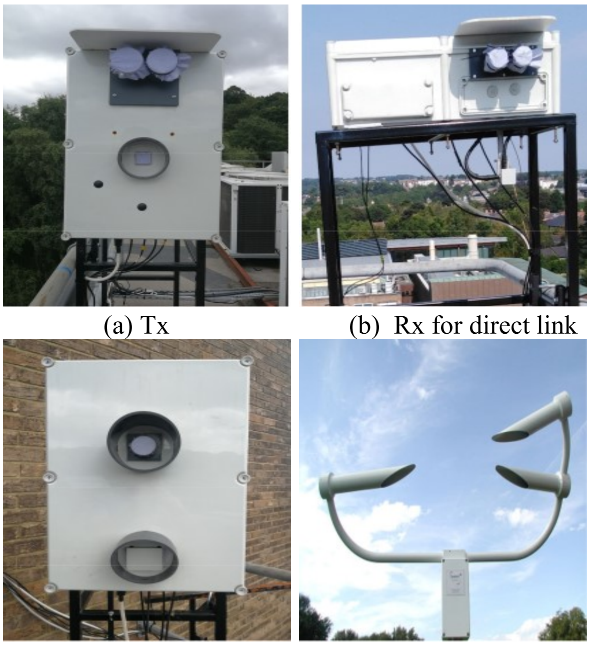

(a) Tx (b) Rx for direct link

(c) Rx for side link (d) Weather station

Figure 1. Tx and Rx boxes.

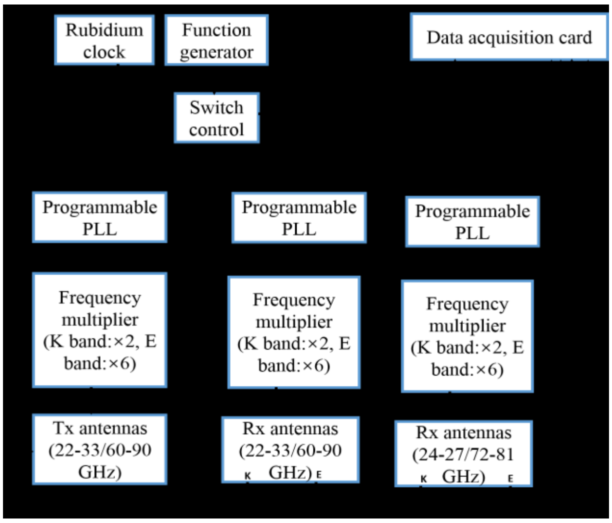

Figure 2. Block diagram of the channel sounder set up.

2.2 *Weather station*

The PWS100 weather station shown in Fig. 1(d) is installed at Durham University, UK within 200 m distance to the link. It is a laser-based sensor which can identify precipitation type and measure the rain rate and DSD. The recorded data include visibility, precipitation intensity, precipitation type, temperature, relative humidity, DSD, etc. The DSD is recorded with 300 values of the number of drops corresponding to the diameter from 0.1 mm to 30 mm with 0.1 mm resolution.

The DSD in unit of $(m^{-3}\ mm^{-1})$ can be calculated as

$$\mathrm{N}(\mathrm{D_i}) = \sum_{j=1}^{300} \frac{\mathrm{n}(\mathrm{D_i}, \mathrm{v_j})}{\mathrm{v_j}} \cdot \frac{1}{\mathrm{S} \cdot \Delta \mathrm{t} \cdot \mathrm{dD_i}} \qquad (1)$$

where S = 40 cm^2 is the measurement surface of the laser beam of the PWS100 disdrometer, t = 60 s is the integration time, n(Di,vj) is the number of particles registered within the classes with mean diameter Di (mm) and mean speed vj (m/s), dDi (mm) is the class width associated with the diameter Di.

3 Rain Attenuation Models

Two models are widely used for rain attenuation. These are the ITU-R P.838-3 model with distance factor and the DSD model with Mie scattering. The ITU model relies on the rain fall rate, while the DSD model with Mie scattering relies on the DSD.

3.1 *ITU-R P.838-3 model*

The ITU model is given as

$$\gamma = k\mathrm{R}^{\alpha} \qquad (2)$$

where R is the rain fall rate (mm/h), k and α are model parameters dependent on the frequency f, and is the specific attenuation in dB/km. The ITU model provides a look-up table for the parameters for different frequencies and polarizations.

The total attenuation for a specific distance depends on the effective path length d_{eff}, between the Tx and Rx antennas is expressed as

$$A = \gamma d_{eff} \qquad (3)$$

where the effective path length, d_{eff}, of the link is obtained by multiplying the actual path length d by a distance factor r, given in the ITU-R P.530-17 model as

$$r = \frac{1}{0.477 d^{0.633} R_{0.01}^{0.073\alpha} f^{0.123} - 10.579(1 - \exp(-0.024d))} \qquad (4)$$

where $R_{0.01}$ is the rain rate exceeded for 0.01% of the time with an integration time of 1 minute.

3.2 *DSD model and Mie scattering*

The DSD model is given as

$$\gamma = 4.343 \times 10^3 \int_0^\infty \delta_{ext}\,(D) N(D) dD \qquad (5)$$

where γ is the specific attenuation in dB/km, $\delta_{ext} = \pi(\frac{D}{2})^2 Q_{ext}$ is the extinction cross section (m^2) for water drops of diameter *D* (mm), and *N(D)* is the drop size distribution value ($m^{-3}\,mm^{-1}$) at diameter *D*. The extinction efficiency Q_{ext} can be calculated from Mie scattering or Rayleigh scattering theory depending on the size parameter x = π D/λ, where λ is the wavelength. The complex water refractive indices, at an average temperature 5°C, at 25.84 GHz and 77.52 GHz are 5.1253+2.7265i and 3.5330+1.6724i, respectively.

4 Results and Analysis

Four rain events and rain attenuation measurements were recorded during 5-18 December 2019. The measurement results are shown in Fig. 3 for the direct and side links. The relative signal levels are compared to sunny days.

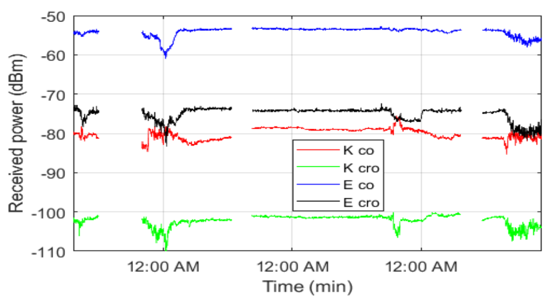

(a) Direct link

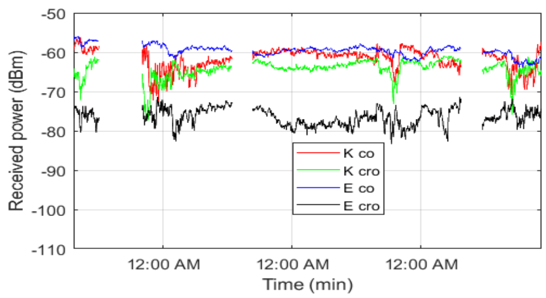

(b) Side link

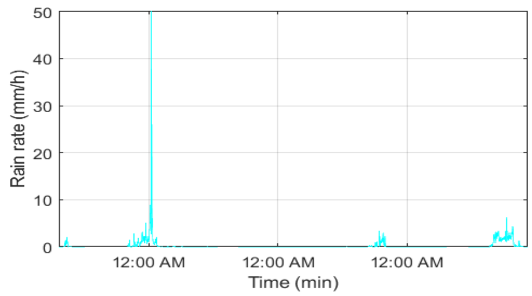

(c) Rain rate

Figure 3. Direct and side link rain attenuations at K and E band.

For the direct link, the attenuation follows the trend of rain for both bands since there is a strong LOS component. For the side link, it relies on NLOS reflected paths to receive the signal and the attenuation can be impacted by scattering from the rain. The mapped received signal in dBm against the rain rate in mm/h shows a correlation between rain rate and rain attenuation for both links with the side link exhibiting higher attenuation than the direct link.

The cross polarization shows higher attenuation for both bands and both links. An accurate modeling of the side link rain attenuation is possible by finding the propagation paths through methods such as wideband channel measurement and ray tracing simulation.

The rain attenuation calculated from the ITU-R P.838-3 model and the DSD model for both bands for the direct link vertical polarizations are shown in Fig. 4. As can be seen, both models are in good agreement.

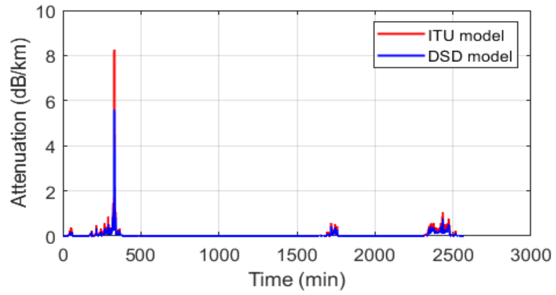

(a) Modeled rain attenuation at K band

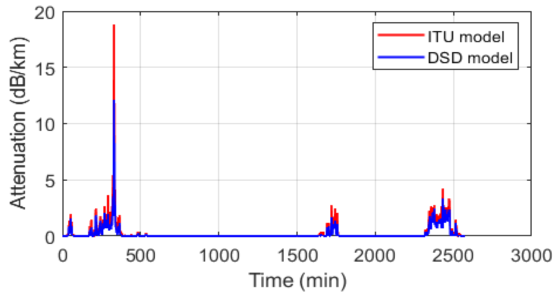

(b) Modeled rain attenuation at E band

Figure 4. Modeled rain attenuation at K band and E band.

When converting the calculated rain attenuations to the specific path length, the distance factor should be considered, as rain is not uniformly distributed in space. Since the empirical equation for the distance factor is mainly derived from long-range measurement datasets, the recommended maximum value of 2.5 is not appropriate for short-range links [13]. The calculated distance factor without the maximum value constraint is applied for the short-range link. Fig. 5 shows the comparison of measured and modeled rain attenuations at K band for the direct link. The measured attenuation is larger than the ITU model and DSD model due to the wet antenna effect (WAE), especially for a short-range link. The model used to estimate the WAE is given as

$$A_a = C(1 - e^{-dA_m^n}) \quad (6)$$

where A_m is the measured attenuation, A_a is the attenuation from WAE, C, d, and n are the fitting parameters [14].

For the direct link in the K band, the fitting parameters are $C = 10$, $d = -0.07$, and $n = 1.2$. The estimated attenuation from the WAE is shown in Fig. 5(a). After removing the WAE from the measurements, the measured attenuation matches well with the predicted attenuation by the ITU model, as shown in Fig. 5(b).

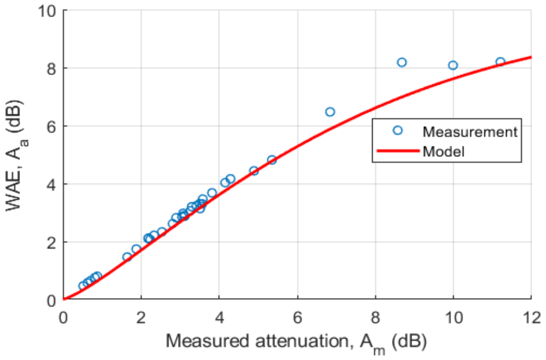

(a) Estimation of WAE

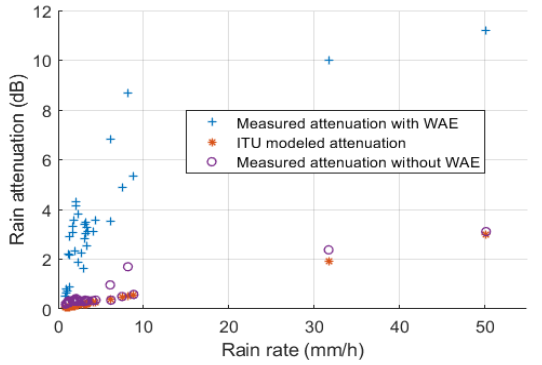

(b) Comparison of measured and estimated rain attenuations

Figure 5. Measured and modeled rain attenuation for K band direct link.

5 Conclusions

In this paper, we have conducted rain attenuation measurements at two mmWave bands for both direct and side links. The PWS100 disdrometer and custom-designed channel sounder have been used to collect weather data and channel data, respectively. The ITU-R P.838-3 model and DSD model were used to model the rain attenuation. The rain attenuation for the direct and side links have been investigated. The side link is shown to have larger attenuation, thus is more challenging for fixed link rain attenuation modeling.

6 Acknowledgements

The authors would like to acknowledge the support of WaveComBE project, under Horizon 2020 research and innovation program with grant agreement No. 766231, the support from Ofcom under grant No. 1362, and the electronics and mechanical workshop technicians at Durham University for the setup of the link.

7 References

1. J. Hansryd, Y. Li, J. Chen, and P. Ligander, "Long term path attenuation measurement of the 71–76 GHz band in a 70/80 GHz microwave link," in *Proc. EuCAP'10*, Barcelona, Spain, Apr. 2010, pp. 1–4.

2 V. Kvicera, M. Grabner, and O. Fiser, "4-year hydrometeor attenuation statistics obtained at 93 GHz on an 850 m terrestrial path," in *Proc. EuCAP'11*, Rome, Italy, Apr. 2011, pp. 2501–2503.

3. M. Schleiss, J. Rieckermann, and A. Berne, "Quantification and modeling of wet-antenna attenuation for commercial microwave links," *IEEE Geosci. Remote Sens. Lett.*, **10**, 5, pp. 1195–1199, Sept. 2013.

4. E. S. Hong, S. Lane, D. Murrell, N. Tarasenko, and C. Christodoulou, "Terrestrial link rain attenuation measurements at 84 GHz," in *Proc. USNC-URSI NRSM'17*, Boulder, CO, 2017, pp. 1–2.

5. E. S. Hong, S. Lane, D. Murrell, N. Tarasenko, C. Christodoulou, and J. Keeley, "Estimating rain attenuation at 72 and 84 GHz from raindrop size distribution measurements in Albuquerque, NM, USA," *IEEE Geosci. Remote Sens. Lett.*, **16**, 8, pp. 1175–1179, Aug. 2019.

6. F. J. A. Andrade, A. A. M. de Medeiros, and L. A. R. da Silva Mello, "Short-term rain attenuation predictor for terrestrial links in tropical area," *IEEE Antennas Wireless Propag. Lett.*, **16**, pp. 1325–1328, May 2017.

7. I. Shayea, T. Abd. Rahman, M. Hadri Azmi, and M. R. Islam, "Real measurement study for rain rate and rain attenuation conducted over 26 GHz microwave 5G link system in Malaysia," *IEEE Access*, **6**, pp. 19044–19064, Mar. 2018.

8. L. Luini, G. Roveda, M. Zaffaroni, M. Costa, and C. Riva, "EM wave propagation experiment at E band and D band for 5G wireless systems: Preliminary results," in *Proc. EuCAP'18*, London, UK, Apr. 2018, pp. 1–5.

9. M. Fencl, P. Valtr, M. Kvicera, and V. Bares, "Quantifying wet antenna attenuation in 38-GHz commercial microwave links of cellular backhaul*," IEEE Geosci. Remote Sens. Lett.*, **16**, 4, pp. 514–518, Apr. 2019.

10. P. Valtr, M. Fencl, and V. Bares, "Excess attenuation caused by antenna wetting of terrestrial microwave links at 32 GHz," *IEEE Antennas Wireless Propag. Lett.*, **18**, 8, pp. 1636–1640, Aug. 2019.

11. C. Han and S. Duan, "Impact of atmospheric parameters on the propa-gated signal power of millimeter-wave bands based on real measurement data," *IEEE Access*, **7**, pp. 113626–113641, Aug. 2019.

12. S. Salous, Y. Cao, and X. Raimundo, "Impact of precipitation on millimetre wave fixed links," in *Proc. EuCAP'19*, Krakow, Poland, Apr. 2019, pp. 1–4.

13. J. Huang, Y. Cao, X. Raimundo, A. Cheema, and S. Salous, "Rain statistics investigation and rain attenuation modeling for millimeter wave short-range fixed links*," IEEE Access*, **7**, pp. 156110–156120, Oct. 2019.

14. M. M. Z. Kharadly and R. Ross, ''Effect of wet antenna attenuation on propagation data statistics,'' IEEE Trans. Antennas Propag., vol. 49, no. 8, pp. 1183–1191, Aug. 2001.